Epigenomics

ISSN: 1750-1911 (Print) 1750-192X (Online) Journal homepage: www.tandfonline.com/journals/iepi20

Exosome-transmitted microRNA-323a-3p participated in the occurrence of Hirschsprung's disease

Haoran Shen, Chenglong Wang, Xiurui Lv, Zichuan Gao, Yuanxiang Qiu, Zhengke Zhi, Jie Tang, Chunxia Du, Ruyi Zhang, Hongxing Li & Weibing Tang

To cite this article: Haoran Shen, Chenglong Wang, Xiurui Lv, Zichuan Gao, Yuanxiang Qiu, Zhengke Zhi, Jie Tang, Chunxia Du, Ruyi Zhang, Hongxing Li & Weibing Tang (29 Mar 2026): Exosome-transmitted microRNA-323a-3p participated in the occurrence of Hirschsprung's disease, Epigenomics, DOI: 10.1080/17501911.2026.2647714

To link to this article: https://doi.org/10.1080/17501911.2026.2647714

EPIGENOMICS
https://doi.org/10.1080/17501911.2026.2647714

RESEARCH ARTICLE

Exosome-transmitted microRNA-323a-3p participated in the occurrence of Hirschsprung's disease

Haoran Shen[a,b], Chenglong Wang[a]*, Xiurui Lv[c]*, Zichuan Gao[a], Yuanxiang Qiu[a], Zhengke Zhi[a], Jie Tang[a], Chunxia Du[a], Ruyi Zhang[a], Hongxing Li[a] and Weibing Tang[a]

[a]Department of Neonatal Surgery, Children's Hospital of Nanjing Medical University, Nanjing, Jiangsu, China; [b]School of Pediatrics, Nanjing Medical University, Nanjing, Jiangsu, China; [c]Department of Pediatric Oncology, Dana-Farber Cancer Institute, Harvard Medical School, Boston, MA, USA

ABSTRACT

Background: Hirschsprung's disease (HSCR) is caused by defective enteric neural crest cell (ENCC) migration. Exosome-transmitted microRNAs are implicated in HSCR pathogenesis, but mechanisms remain unclear.

Methods: Plasma exosomes and colon tissues were collected from HSCR patients and controls. We assessed the effects of exosomal miR-323a-3p on the proliferation and migration of immortalized ENCC-derived neural cell line (iENC) in vitro using CCK-8, EdU and Transwell assays, and its impact on ENCC migration in vivo using a zebrafish model.

Results: Exosomal miR-323a-3p was significantly upregulated in the plasma of HSCR and exhibited prospective diagnostic relevance (AUC = 0.7269, $p = 0.0043$). Exosomal miR-323a-3p was taken up by iENCs and suppressed their proliferation and migration. TET2 was identified as a potential miR-323a-3p target. TET2 was downregulated in HSCR aganglionic tissues, and its knockdown inhibited iENC proliferation and migration. In the zebrafish model, exosomal miR-323a-3p impaired distal ENCC colonization.

Conclusion: Exosomal miR-323a-3p is upregulated in HSCR and associated with impaired ENCC-derived cell function, potentially via TET2. These findings suggest exosome-transmitted microRNA-323a-3p participated in the occurrence of Hirschsprung's disease and exhibit promising potential as a prospective diagnostic biomarker.

PLAIN LANGUAGE SUMMARY

Hirschsprung's disease (HSCR) is a birth disorder caused by missing nerve cells in the gut. In this study, we discovered that small particles called exosomes carry a molecule named miR-323a-3p that is found at higher levels in the blood of HSCR patients. This molecule slows down the growth and movement of key nerve cells in the intestine. We also found that miR-323a-3p potentially does this by blocking TET2, a gene important for nerve development. Our results suggest that measuring plasma exosomal miR-323a-3p in blood could help doctors diagnose HSCR earlier and that the miR-323a-3p/TET2 pathway may be a target for future treatments.

ARTICLE HISTORY
Received 16 May 2025
Accepted 16 March 2026

KEYWORDS
Hirschsprung's disease; exosomes; microRNAs; enteric nervous system; neural crest cells

1. Introduction

Hirschsprung's disease (HSCR) is a life-threatening congenital disorder caused by defective migration of enteric neural crest cells (ENCC), leading to aganglionosis in the distal gut [1]. Current HSCR treatment relies on surgical resection of aganglionic bowel [2]. While lifesaving, this approach frequently leads to chronic complications such as enterocolitis, growth impairment, and bowel dysfunction [3]. Elucidating the molecular pathogenesis of HSCR is thus critical for developing targeted therapies to improve early diagnosis and long-term outcomes. It is worth noting that emerging evidence challenges the conventional gene-centric view of HSCR pathogenesis. Beyond elucidated protein-coding genes, including RET, GDNF, SOX10, EDNRB, emerging evidence highlights microRNAs (miRNAs) as key regulators in HSCR pathogenesis [4,5]. It has been reported that miRNAs such as miR-142-3p, miR-637 and miR-424 serve as key developmental effectors within the enteric nervous system (ENS), which are involved in regulating the proliferation, migration and differentiation of ENCC [6–8].

Exosomes are nanovesicles of bilayer lipid membranes, which encapsulate various biologically active molecules, and can mediate communication between cells and participate in various pathophysiological processes [9,10]. Recent studies reveal that regulatory miRNAs can be shuttled between cells via exosomes, particularly exosomes, establishing a novel intercellular communication network in early nervous system development [11–13]. In addition, exosomal miRNAs have good potential as noninvasive biomarkers, given the stability of their contents, tissue specificity and ubiquity in body fluids [14,15]. However, at present, the research on exosomal miRNAs in neural development mainly

CONTACT Hongxing Li hx8817@126.com; Weibing Tang twbcn@njmu.edu.cn Department of Neonatal Surgery, Children's Hospital of Nanjing Medical University, 72 Guangzhou Road, Nanjing, Jiangsu 210008, People's Republic of China
*The authors contributed equally to this work.

Supplemental data for this article can be accessed online at https://doi.org/10.1080/17501911.2026.2647714

Article highlights

- Plasma exosomal miR-323a-3p is significantly upregulated in Hirschsprung's disease (HSCR) patients and shows diagnostic potential.
- Exosomal miR-323a-3p inhibits proliferation and migration of immortalized ENCC-derived neural cell line (iENC) *in vitro*.
- TET2 is identified as a potential target of miR-323a-3p and is downregulated in HSCR aganglionic tissues.
- Knockdown of TET2 impairs iENC proliferation and migration, consistent with the effects of miR-323a-3p overexpression.
- In vivo zebrafish experiments confirm that exosomal miR-323a-3p disrupts the colonization of enteric neural cells to the distal segment.

focuses on the field of central nervous system diseases, while there are relatively few reports on the enteric nervous system, especially in HSCR.

Our previous study has identified five significantly and steadily altered exosomal miRNAs in HSCR plasma through high-throughput Illumina sequencing and RT-qPCR. Among which, miR-323a-3p was markedly upregulated in HSCR and demonstrated potential to participate in the pathological mechanism and serve as a biomarker of HSCR [16]. While miR-323a-3p has been shown to inhibit tumor growth through ErbB3/EGFR signaling and attenuate pulmonary fibrosis via TGF-α/β pathways [17,18], its function in enteric nervous system development and Hirschsprung's disease pathogenesis remains unknown. In this study, we investigated that exosomal miR-323a-3p participated in the pathogenesis of HSCR by targeting TET2 to inhibit the proliferation and migration of ENCC, and evaluated its potential as a biomarker for HSCR.

2. Materials and methods

2.1. Study design and sample collection

This study collected plasma samples, aganglionic colonic tissues and normal tissues from 29 patients with HSCR and 25 healthy controls without abnormal development of the enteric nervous system admitted to the Children's Hospital of Nanjing Medical University (Certification No:202411007-1). HSCR diagnoses were confirmed via biopsy after surgery. Patients with other pathological factors that might interfere with plasma exosomal miRNA production were excluded, such as severe cardiovascular diseases, immune diseases, and other serious hereditary diseases. All plasma and tissue samples, once collected, were immediately stored at −80°C until use.

2.2. Cell culture and transfection

Human 293T cell lines were purchased from American Type Culture Collection (ATCC, USA). 293T cells were cultivated in Dulbecco's Modified Eagle medium (DMEM) (Hyclone, USA) mixed with 10% heat-inactivated fetal bovine serum (FBS), 100 U/ml of penicillin, and 100 µg/ml of streptomycin under 5% CO_2 at 37°C.

Mouse embryonic primary enteric neural crest cells (ENCC) were isolated from C57BL/6J mice for 14.5–16.5 gestational days provided by the Animal Core Facility of Nanjing Medical University. Fetal mice were obtained from anesthetized pregnant dams, and their intestinal tracts were dissected and the mesentery carefully removed under an anatomical microscope. The intestinal tissue was cut into 1 mm^3 pieces and dissociated with collagenase IV (C5138-25 MG, Sigma, USA) at 37°C for 30 min, followed by 70-µm filtration and centrifugation (1,000 g, 5 min). The precipitate was resuspended and cultured in neural-specific medium (CM-M216, Procell, China) under 5% CO2 at 37°C. The culture supernatant was collected at the appropriate time and passaged at least three times to obtain purified neurospheres. ENCC-derived neurospheres were identified by immunofluorescence staining for SOX10 and p75.

Immortalized ENCC-derived neural cell line (iENC) was established in accordance with the following methods. ENCC were infected with SV40 immortalization lentivirus (Applied Biological Materials, Canada), enabling stable passage for more than 20 generations. Successful establishment was confirmed by immunofluorescence detection of neural precursor markers (p75 and Nestin) and neuronal markers (Calretinin and PGP9.5). The plasmids encoding miR-323a-3p mimics, miR-323a-3p inhibitors, TET2 overexpression, TET2 siRNA and the matching control plasmids were synthesized by Genechem (China). Plasmids transfection was performed using Lipofectamine 3000 (Invitrogen, USA) in accordance with the manufacturer's instructions.

2.3. Isolation, identification and co-culture of exosomes

The exosomes from plasma and cell medium (CM) were isolated as following methods. Plasma exosomes were isolated using exosome precipitation solution (System Biosciences, USA). Each sample was mixed with 4 µl of Thrombin per 0.5 ml plasma and the mixture was incubated at room temperature for 5 min. After centrifugation at 10000rpm for 5 min in a standard microfuge, at the bottom of the tube was a visible fibrin pellet and the supernatant was transferred to another tube and filtered with 0.22-µm PVDF filters (Millipore, USA). Then, exosomes precipitation solution (System Biosciences) was added into the plasma-like supernatant before refrigeration for 30 min at 4°C. Subsequently, the/plasma mixture was centrifuged at 1500 g for 30 min, and the exosomes were obtained at the bottom of the vessel as a white or beige pellet.

The CM of 293T cells was centrifuged for 20 min (500 g) to remove cell debris, and then the supernatant was transferred to a new clean centrifuge tube, centrifuged at 10,000 g for 30 min, and filtered using a 0.22 µm PVDF filter (Millipore) to obtain the CM pretreatment solution. Exosomes were further isolated from CM pretreated supernatants based on molecular size exclusion chromatography (SEC) using the exosomes purification kit (Echo Biotech, China) of appropriate specifications, and then concentrated and purified using 100 kDa ultrafiltration tubes (Millipore, USA).

Isolated exosomes were diluted in 100 µl of PBS and fixed with 5% glutaraldehyde and then kept at 4°C until TEM analysis. According to the TEM sample preparation protocol, a drop of exosomes sample was placed on the carbon-coated copper grid, and then immersed in 2% phosphotungstic acid solution (pH 7.0) for 30 s. Transmission electron microscope (Tecnai G2 Spirit Bio TWIN, FEI, USA) was adopted to obtain the microphotographs.

Meanwhile, nanoparticle tracking analysis (NTA) was conducted for the isolated exosomes with Zetasizer Nano ZS90 (Malvern Instruments, UK) and with its corresponding software.

The concentration of exosomes in the isolated cell CM was detected using the BCA Protein Assay Kit (Beyotime, China) and co-cultured with the recipient cells at a concentration of 20 μg/ml. To observe the cellular uptake of exosomes, the purified exosomes were labeled using the PKH67 (MedChemExpress, USA). After co-culturing the receptor cells iENC with the labeled exosomes for 4 h, the cells were fixed and stained with Hochest 33,432. Photos were taken using a Leica STELLARIS 5 laser scanning confocal microscope (Leica, Germany).

2.4. Protein preparation and western blot

Isolated exosomes were resuspended in RIPA-PMSF Buffer to obtain the total protein of exosomes. The BCA Protein Assay Kit (Beyotime, China) was utilized in accordance to manufacturer's instructions to determine the protein concentration. Protein of each exosomes sample was separated on a 10% SDS-PAGE gel and transferred to a polyvinylidene fluoride membrane, before getting blotted with antibodies against CD9 (ab92726, Abcam, USA), and CD63 (ab134045, USA), respectively. Eventually, ECL reagent kit (Millpore, Billerica, MA) was used to detect the target protein.

2.5. RNA extraction and RT-qPCR

Cell/Tissue Total RNA Isolation Kit (Vazyme, China) was employed to extract the total RNA following manufacturer's instructions. NanoDrop 2000 Spectrophotometer (Thermo Scientific, USA) was utilized for RNA quantity control and determining RNA concentration. For microRNA, cel-miR-39 (RiboBio, China) was added as external control. TaqMan microRNA Reverse Transcription Kit (Applied Biosystems, USA) and microRNA-specific stem-loop primers (Applied Biosystems, USA) were used to reverse transcribe the total RNA, and the real-time quantitative PCR was conducted in accordance to the guidelines of the TaqMan miRNA assay (Applied BioSystems, USA). Each reverse transcription product was mixed with the TaqMan Universal PCR master mix and its corresponding probe mix before incubation at 95°C for 10 min, followed by 40 cycles of 94°C for 15 s and 60°C for 1 min. For mRNA, we adopted the Reverse Transcription Kit (Takara, Japan) and SYBR Premix Ex Taq (TaKaRa, China). GAPDH was used as an endogenous control for mRNA. The relative expression level was analyzed using the $2^{-\Delta\Delta CT}$ method. All primers are listed in Table S1.

2.6. Cell proliferation assay

Cell Counting Kit-8 (CCK-8) (APExBIO, USA) and EdU Cell Proliferation Kit with AF594 EdU (Beyotime, China) assay were performed based on the manufacturer guidelines to examine cell proliferation. For CCK8 assay, the counted 5×10^3 iENC were cultured in 96-well plates for 12, 24, 48 and 72 h respectively, and then incubated in CCK8 for 1 h. The absorbance was measured at 450 nm using BioTek Synergy H1 Multifunctional Microplate Detector (Agilent, USA). For EdU assay, EdU solution was added into iENC for incubation at 37°C for 2 h. The cells were then fixed with 4% paraformaldehyde for 30 min and stained using 1× reaction cocktail for 30 min before incubation with Hoechst 33,342 for 30 min. Using the Leica STELLARIS 5 laser scanning confocal microscope (Leica, Germany), 20 random fields of view were selected to calculate the number of Edu-positive cells.

2.7. Cell migration assay

Transwell assay was utilized to measure the ability of cell migration. The counted 2×10^4 cells were seeded into the upper compartment of the transwell apparatus (Corning, USA) in plasma-free medium. The lower compartment was enriched with complete medium supplemented with 10% fetal bovine plasma (FBS). Following a 24-h incubation period, the cells that had migrated were immobilized with 4% paraformaldehyde (PFA) and subsequently stained with crystal violet. Images of the migrated cells were obtained through inverted microscope (OLYMPUS, Japan).

2.8. Dual-luciferase reporter assay

Firefly luciferase gene reporter plasmid including GV272-TET2-WT, GV272-TET2-MUT, TK renilla luciferase reporter plasmid, miR-323a-3p mimics, and corresponding control plasmids were constructed by Genechem (China). iENC was cultured in 24-well plates until the cell density was 70–80%. Each well was co-transfected with 1 μg of miR-323a-3p mimics or negative controls, 1 μg of GV272-TET2-WT or GV272-TET2-MUT, and 100 ng of renal luciferase plasmids using Lipofectamine 3000 reagent (Invitrogen, USA). The luciferase activity was measured using the dual-luciferase reporter assay kit (MCE, USA).

2.9. Zebrafish model

The Tg(HuC/D:tdTomato) zebrafish model, developed by Hunter Biotech (Nanjing, China), was used, which integrates the HuC/D neuronal marker with the tdTomato reporter (red fluorescence) via genetic fusion, allowing specific visualization of neurons. Single-cell stage zebrafish embryos were microinjected with NC-exo or miR-323a-OE-exo and harvested at 120 h post-fertilization (hpf). For fluorescence imaging, embryos were permeabilized with 1% Triton X-100 for 5 min, rinsed with cold ddH_2O, and imaged using a stereofluorescence microscope (Leica STELLARIS 5, Germany). Using this model, we visualized enteric neural signals located dorsally to the yolk sac and closely ventral to the spinal cord. These signals originated from HuD-protein-expressing neuronal or neuronal precursor cells distributed in a tubular structure extending along the anterior-posterior axis and appeared as granular, discrete fluorescence along the intestinal tract. Based on the tdTomato fluorescence derived from HuC/D-positive enteric neurons, the proportion of nerve cells that successfully colonized from the intestine to the cloaca was quantified.

2.10. Statistical analysis

Statistical analyses were performed using ImageJ 1.8.0, SPSS 23.0, and GraphPad Prism 9.0. Data are presented as mean ± SD, as

specified in the figures. Comparisons between two groups were performed using independent samples Student's t-tests. Variance homogeneity was assessed prior to analysis using F-test, and the t-test was applied with the appropriate assumption of equal or unequal variances. All experiments were independently repeated at least three times, and statistical significance was defined as $p < 0.05$.

3. Results

3.1. Characterization of plasma and CM derived exosomes

The isolated exosomes from plasma and CM were characterized using three methods. Transmission electron microscopy was utilized to visualize the exosomes, and membrane-bound exosomes of typical sizes were captured (Figure 1(A)). Then the size distribution of the exosomes isolated in each manner was detected via nanoparticle tracking analysis, which also validated the presence of vesicles of 40–100 nm (Figure 1(B)). Western blot analysis showed that the presence of exosomes markers CD9 and CD63 in both plasma and CM-derived exosomes (Figure 1(C)). These results are consistent with the previously reported characteristics of exosomes and demonstrate the feasibility of isolating exosomes using the aforementioned methods.

3.2. The expression of plasma-derived exosomal miR-323a-3p is upregulated in patients with HSCR

Our previous study has detected high expression levels of miR-323a-3p in HSCR plasma derived exosomes [16]. We examined the stability of exosomal miR-323a-3p under room temperature storage conditions and found that the expression level of miR-323a-3p did not change significantly within 48 h of room temperature storage (Figure 1(D)). Further verification revealed that exosomal miR-323a-3p levels were significantly elevated in patients with HSCR compared with normal control subjects ($p = 0.0073$) (Figure 1(E)). Receiver operating characteristic (ROC) curve analysis indicated that exosomal miR-323a-3p showed the potential diagnostic value for HSCR (AUC = 0.7269, $p = 0.0043$) (Figure 1(F)).

3.3. miR-323a-3p impairs cell proliferation and migration of iENC

To investigate the biological function of miR-323a-3p in the pathogenesis of HSCR, primary enteric neural crest cells (ENCC) were first

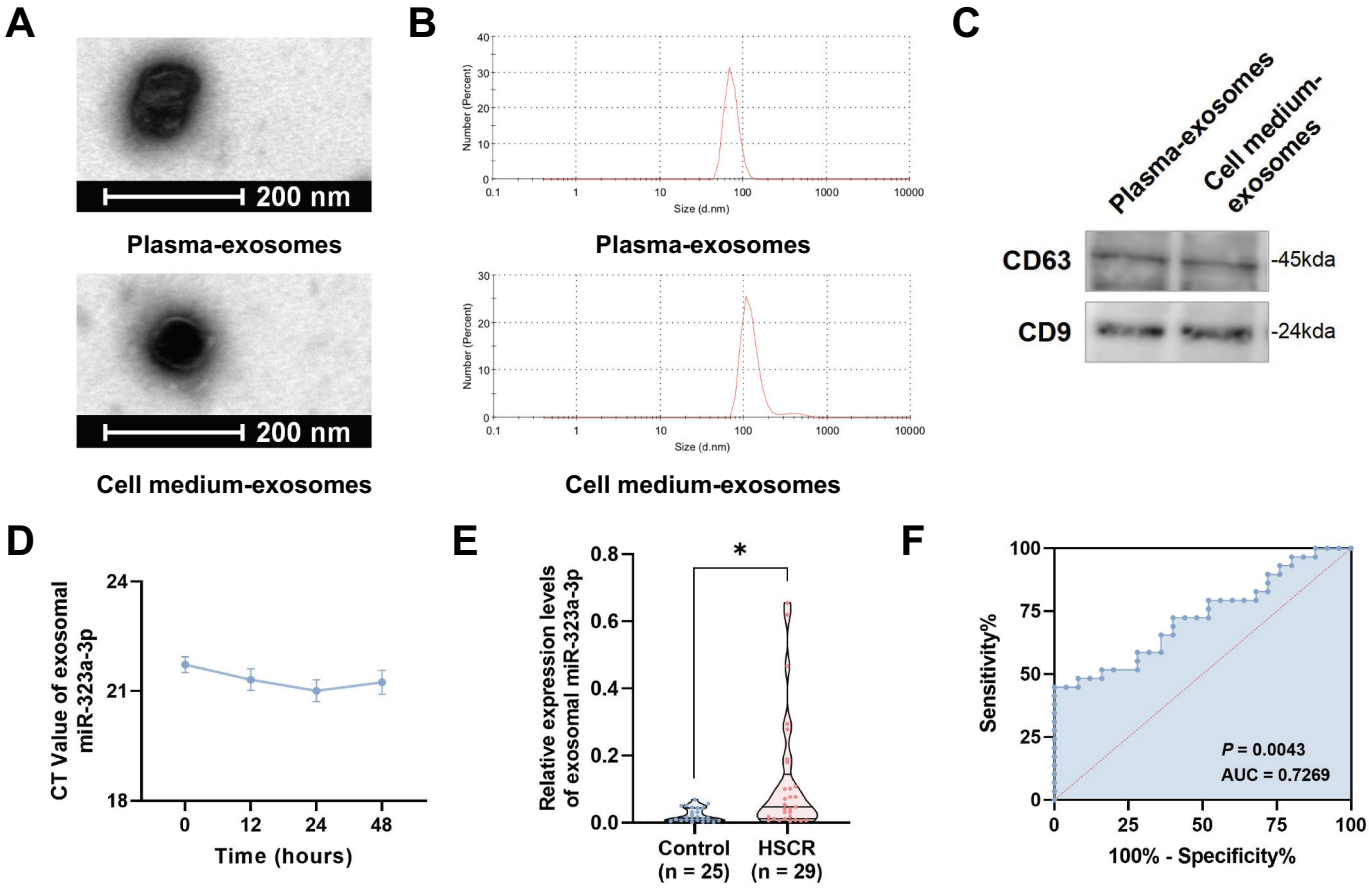

Figure 1. Characterization of exosomes and miR-323a-3p expression profile in HSCR. (A) Transmission electron microscopy (TEM) images showing membrane-bound vesicles with typical exosomes morphology (scale bars = 200 nm). (B) Nanoparticle tracking analysis (NTA) demonstrating size distribution (40–100 nm) of exosomes isolated from plasma and cell medium. (C) Western blot analysis confirming the presence of positive exosomes markers including CD9 and CD63 in both plasma and cell medium (CM) derived exosomes. (D) Stability of the expression level of exosomal miR-323a-3p at room temperature over time detected by RT-qPCR. (E) The expression level of exosomal miR-323a-3p derived from HSCR plasma was upregulated compared with the control group detected by RT-qPCR. (F) The ROC curve was plotted to analyze the diagnostic potential of exosomal miR-323a-3p.

isolated and identified from mice (Figure S1) and constructed immortalized intestinal nerve cell lines (iENC), the details of which have been described in the method. Immunofluorescence analyses of p75, Nestin, Calretinin, and PGP9.5 indicated the successful establishment of iENC as an ENCC-derived neural cell line (Figure S2). MiR-323a-3p was overexpressed or knocked down in iENCs via transfection with overexpression plasmids or siRNA (Figure 2(A,B)). Both CCK8 and EdU assay revealed that miR-323a-3p overexpression significantly attenuated iENC cell proliferation while knockdown of miR-323a-3p markedly promoted cell growth (Figure 2(C,D)). Furthermore, Transwell assay disclosed that iENC cell migration was inhibited by upregulation of miR-323a-3p and fostered by downregulation of miR-323a-3p (Figure 2(E)).

3.4. Exosomal miR-323a-3p secreted by 293T cells can be transferred to iENC

293T cells were transfected with miR-323a-3p mimics plasmid and the exosomes were extracted from CM (Figure 3(A)). It was detected that the expression of miR-323a-3p in exosomes derived from miR-323a-3p-overexpressed 293T cells (abbreviated as miR-323a-3p-OE-exo) was significantly increased compared with exosomes derived from normal 293T cells (abbreviated as NC-exo) (Figure 3(B)). To characterize the distribution of miR-323a-3p, CM from 293T cells was treated with RNase A alone or in combination with Triton X-100. Quantitative analysis revealed that RNase A treatment alone had no significant effect on extracellular miR-323a-3p levels, whereas co-treatment with Triton X-100 led to a substantial reduction in detectable miR-323a-3p (Figure 3(C)), suggesting that the majority of extracellular miR-323a-3p was not freely secreted but rather packaged within lipid-based exosomes. Exosomes isolated from 293T cell CM were labeled with the lipophilic fluorescent dye PKH67 and co-incubated with iENC cells [19]. After co-incubation with exosomes isolated from miR-323a-3p overexpressed 293T cells (shorted for miR-323a-3p-OE-exosomes) for 4 h, a significant increase in intracellular miR-323a-3p levels was detected in the recipient iENC (Figure 3(D)). In addition, there is a distinct PKH67 fluorescence signal localization in the cytoplasm of iENC (Figure 3(E-F)). These results indicate that the recipient cells successfully internalized 293T-derived exosomes, supporting the functional transfer of exosomal miR-323a-3p.

3.5. Exosomal miR-323a-3p inhibit the proliferation and migration of iENC

To examine whether exosomal miR-323a-3p would interfere with the proliferation and migration of iENC, we conducted functional experiments. It was found that the proportion of proliferating cells in iENC co-cultured with miR-323a-3p-OE-exosomes was significantly reduced quantified by EdU assay

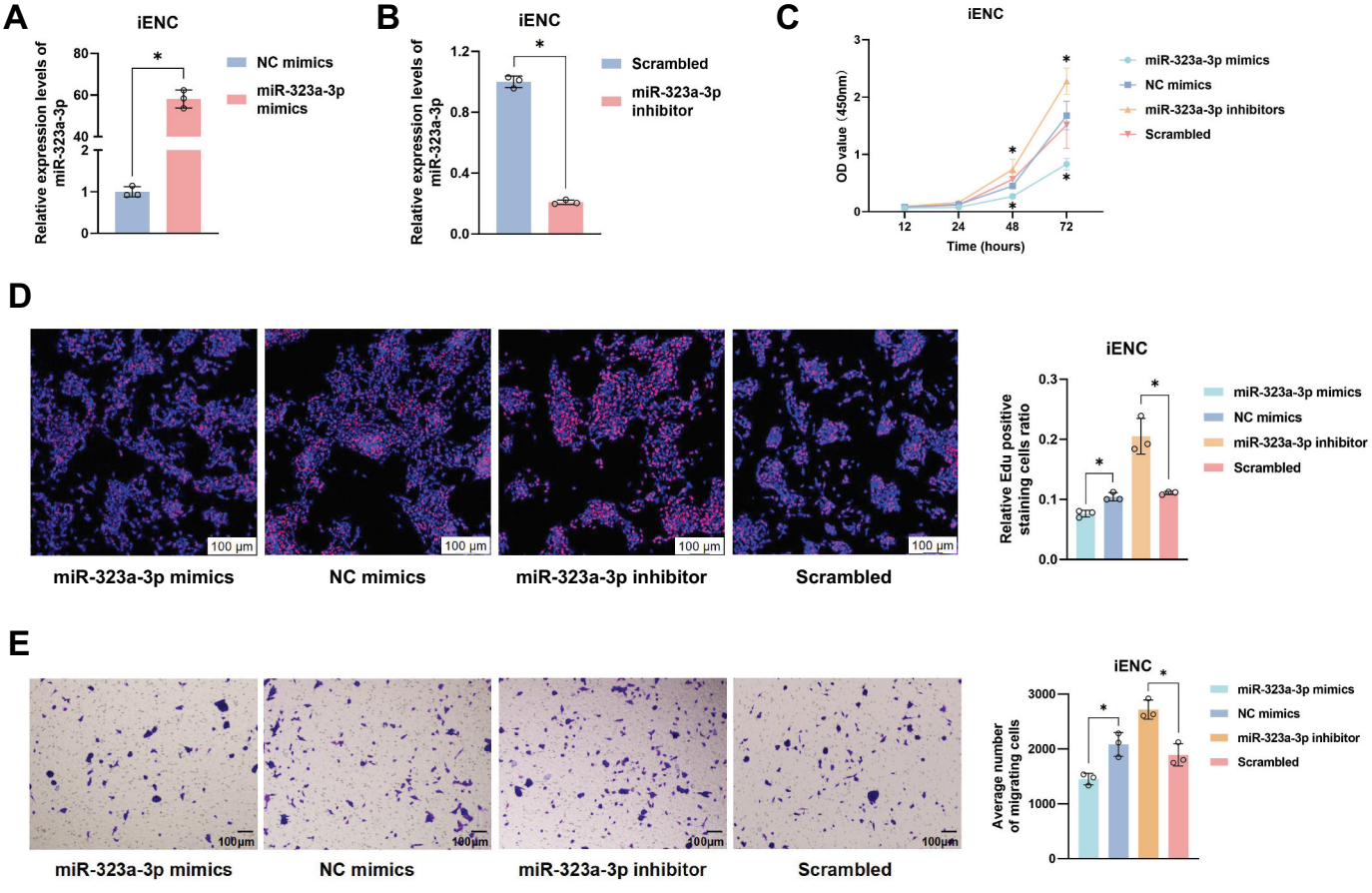

Figure 2. The effect of miR-323a-3p on the proliferation and migration functions of iENC. (A) The overexpression efficiency of miR-323a-3p in iENC detected by RT-qPCR. (B) The knockdown efficiency of miR-323a-3p in iENC detected by RT-qPCR. (C) The CCK-8 assay was used to detect the effect of miR-323a-3p mimics and inhibitor transfection on the proliferation ability of iENC. (D) The Edu assay was used to detect the effect of miR-323a-3p mimics and inhibitor transfection on the proliferation ability of iENC. (E) The transwell migration assay was used to detect the effect of miR-323a-3p mimics and inhibitor transfection on the migeration ability of iENC.

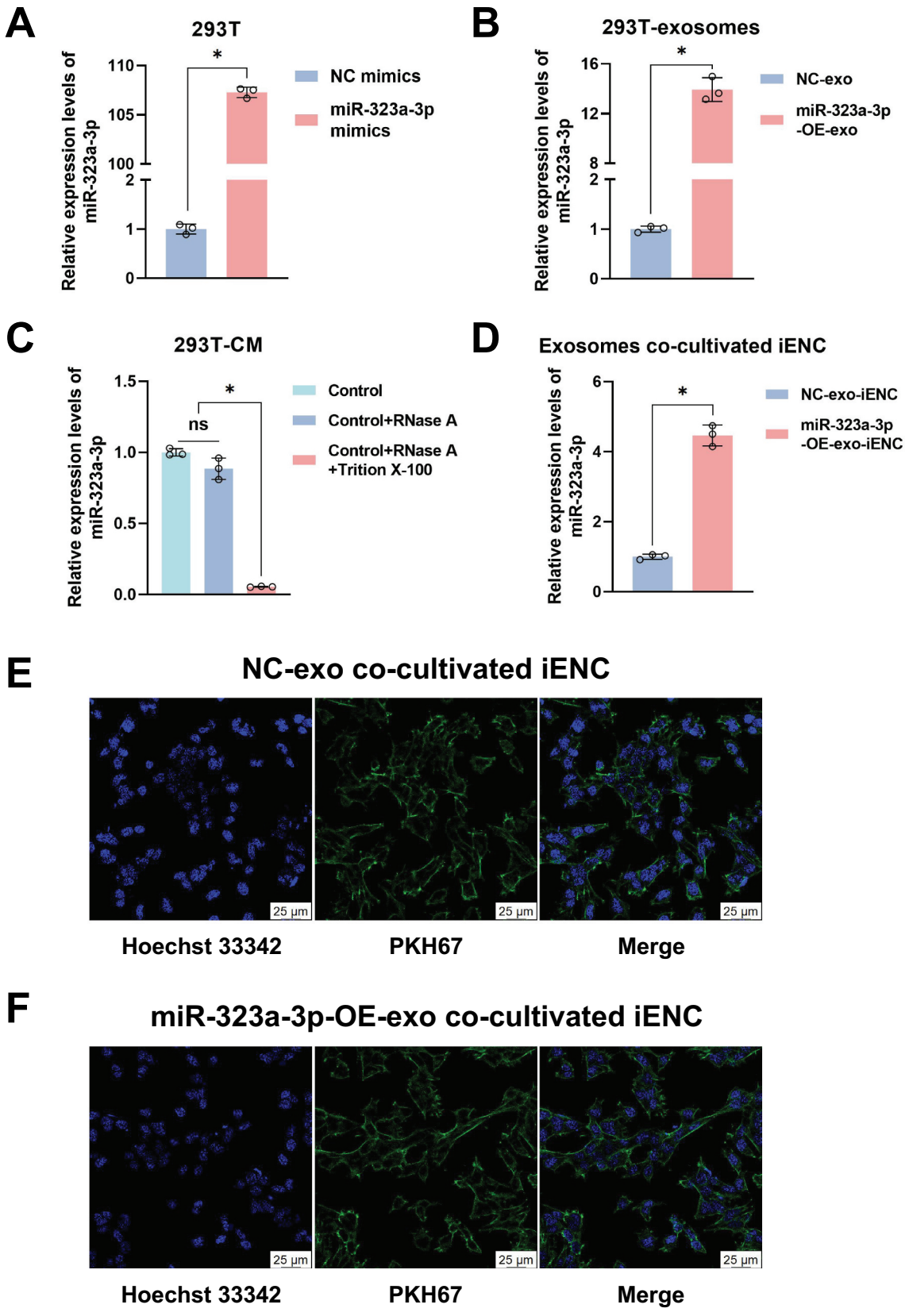

Figure 3. Exosomal miR-323a-3p derived from 293T cells entered iENC. (A) The overexpression efficiency of miR-323a-3p in 293T cells detected by RT-qPCR. (B) The expression levels of miR-323a-3p in exosomes derived from miR-323a-3p overexpressed 293T cells was detected by RT-qPCR. (C) The expression levels of miR-323a-3p in the CM of 293T cells treated with RNase A, RNase A+TritionX-100 and the control was detected by RT-qPCR. (D) The expression levels of miR-323a-3p in the exosomes co-cultivated iENC was detected by RT-qPCR. (E) Confocal microscopy images showed that the PKH67-labeled NC-exosomes (green) were internalized by iENC. (F) Confocal microscopy images showed that the PKH67-labeled miR-323a-3p-OE-exosomes (green) were internalized by iENC.

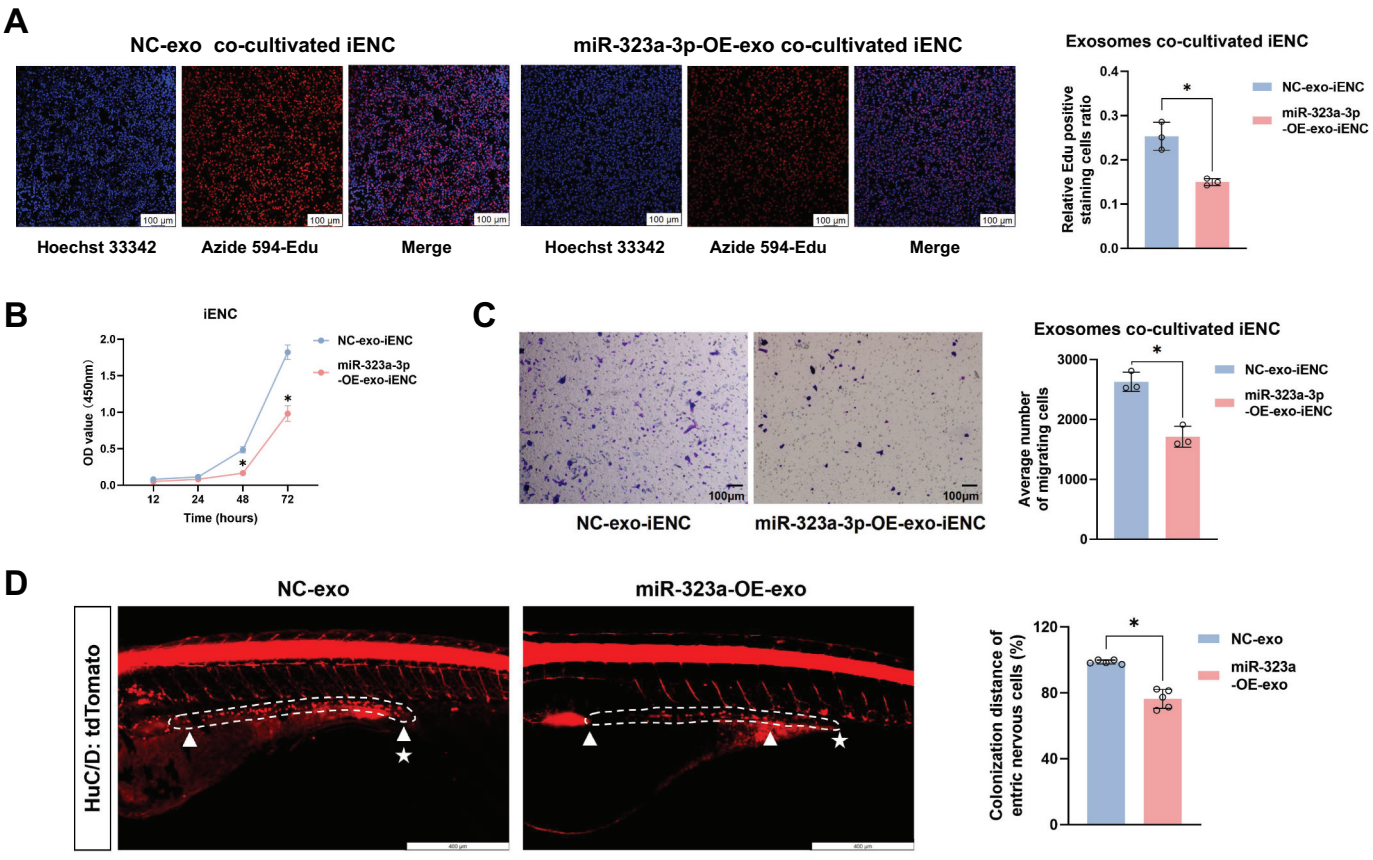

Figure 4. Exosomal miR-323a-3p inhibited the migration function of neural crest cells both in vitro and in vivo. (A) The Edu assay was used to detect the effect of NC-exosomes or miR-323a-3p-OE-exosomes co-cultivation on the proliferation ability of iENC. (B) The CCK-8 assay was used to detect the effect of NC-exosomes or miR-323a-3p-OE-exosomes co-cultivation on the proliferation ability of iENC. (C) The transwell migration assay was used to detect the effect of NC-exosomes or miR-323a-3p-OE-exosomes co-cultivation on the migeration ability of iENC. (D) Fluorescence imaging of the Tg(elavl3:tdTomato) zebrafish intestine was performed to observe the effects of NC-exosomes or miR-323a-3p-OE-exosomes injection on intestinal neural colonization. The extent of the enteric nervous system is demarcated by a white dashed box, with two triangles marking its rostral and caudal boundaries, and a pentagram indicating the position of the cloaca.

(Figure 4(A)). Meanwhile, Transwell and CCK8 experiments demonstrated that the proliferation and migration abilities of miR-323a-3p-OE-exosomes co-cultured cells were significantly weakened (Figure 4(B,C)). In addition, in vivo intestinal fluorescence imaging of Tg(elavl3:tdTomato) transgenic zebrafish injected with miR-323a-3p-OE-exosomes showed impaired distal colonization of colonic neural cells, which failed to reach the cloaca (Figure 4(D)). These findings demonstrated that ENCC-derived neural cells exposed to miR-323a-3p-enriched exosomes may exhibit decreased proliferation and migration, implying a potential role for miR-323a-3p in modulating ENCC-derived cell behavior.

3.6. TET2 is a potential downstream target of miR-323a-3p

To explore the downstream target gene of miR-323a-3p, four distinct prediction tools were employed, and eight genes were jointly identified as potential binding partners of miR-323a-3p, including ARL5A, SEC23B, AUTS2, PPP1CB, TET2, IKZF2, ST7L, KCTD12 (Figure S3). Based on existing literature, both ARL5A and TET2 have been implicated in the regulation of cellular proliferation and migration processes [20–22]. The expression levels of ARL5A and TET2 in control and HSCR tissue samples were detected by RT-qPCR, and it was found that TET2 showed a significant downregulation in HSCR colon tissues (Figure 5(A) and S4). As expected, overexpression of miR-323a-3p led to a significant downregulation of Tet2 mRNA levels in iENC (Figure 5(B)). To validate the regulation interaction between miR-323a-3p and TET2, the luciferase reporter plasmids included predicted (GV272-TET2-WT) or mutant binding sites (GV272-TET2-MUT) were constructed and co-transfected with miR-323a-3p mimics or negative control in 293T cells, respectively. The results indicated suppressed luciferase intensity of the WT reporter after transfection of miR-323a-3p mimics, while no significant change of luciferase activity was detected in the MUT reporter (Figure 5(C)). These findings suggested that TET2 may be a potential target of miR-323a-3p, as indicated by luciferase reporter assay and miR-323a-3p-induced downregulation of TET2 mRNA.

3.7. Downregulation of TET2 impairs proliferation and migration of iENC

To elucidate the functional role of TET2 in HSCR, we modulated TET2 expression in iENC through either plasmid-mediated overexpression or siRNA-mediated knockdown

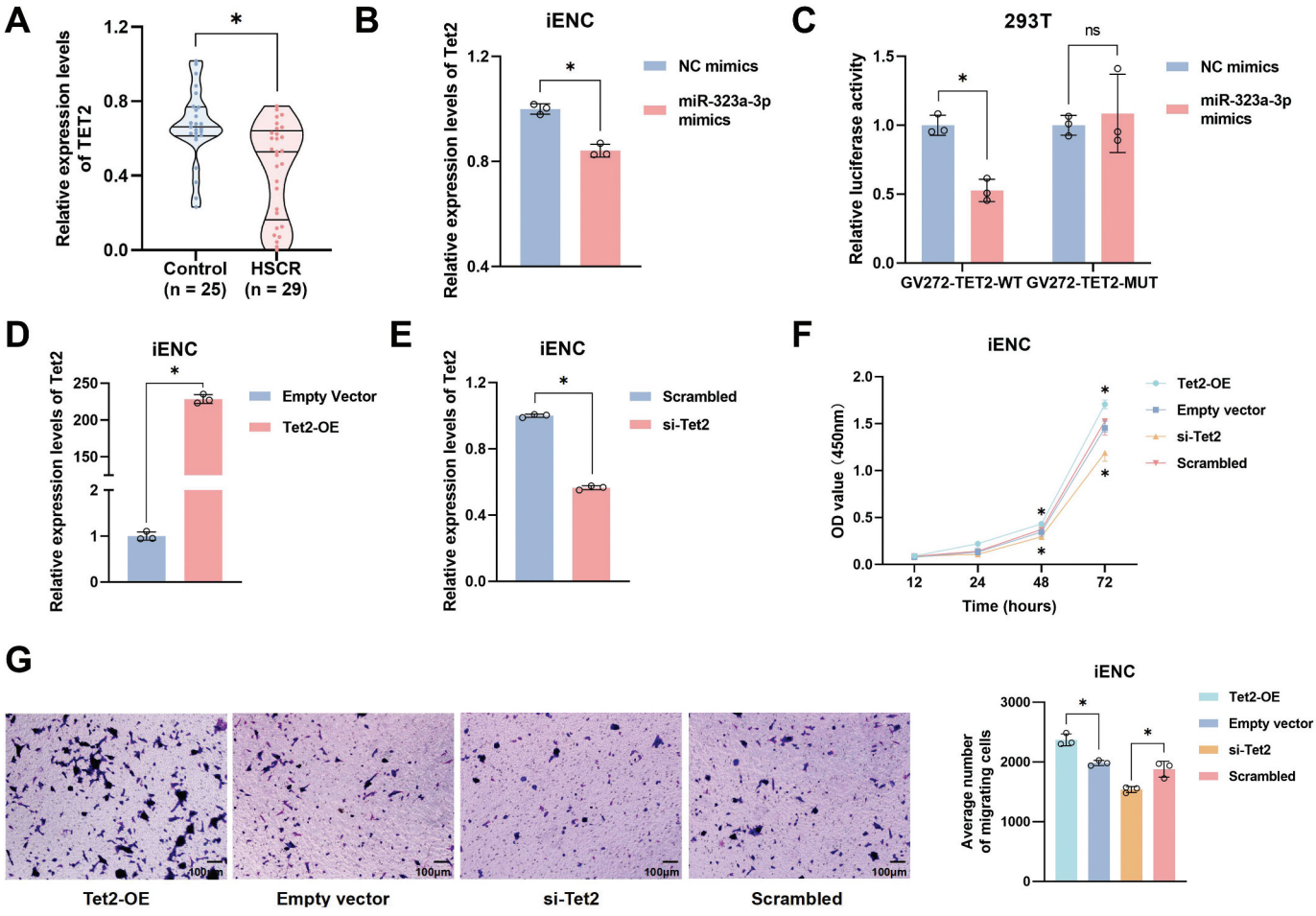

Figure 5. TET2 regulated the proliferation and migration function as a downstream interaction target of miR-323a-3p. (A) The expression level of TET2 in the ganglion tissue of HSCR was downregulated compared with the control group detected by RT-qPCR. (B) The expression levels of Tet2 in miR-323a-3p overexpressed iENC were detected by RT-qPCR. (C) The dual-luciferase reporter assay demonstrated that miR-323a-3p binds to the TET2 3′UTR-WT but not to the MUT in 293T cells. (D) The overexpression efficiency of Tet2 in iENC detected by RT-qPCR. (E) The knockdown efficiency of Tet2 in iENC detected by RT-qPCR. (F) The CCK-8 assay was used to detect the effect of Tet2 overexpression or knockdown on the proliferation ability of iENC. (G) The transwell assay was used to detect the effect of Tet2 overexpression or knockdown on the migeration ability of iENC.

(Figure 5(D–E)). The CCK-8 assay demonstrated that TET2 knockdown markedly inhibited iENC proliferation, whereas TET2 overexpression promoted proliferative activity (Figure 5(F)). Consistent with these findings, Transwell migration assays showed that TET2 silencing significantly attenuated cell migration capacity, while TET2 overexpression enhanced migratory potential (Figure 5(G)). These results suggested that TET2 downregulation was associated with reduced proliferation and migration of iENCs, indicating a potential role in ENCC-related cellular functions. Further studies are needed to determine its contribution to HSCR pathogenesis.

4. Discussion

Exosomes represent a significant type of intercellular communication and serve as vehicles for transfer between cells of membrane and cytosolic protein, RNA, and lipid [23]. Mounting evidence suggests that exosomal cargoes, particularly noncoding RNAs, may play important roles in both physiological development and disease progression [24]. Exosomal miRNAs in body fluid (plasma, urine, etc.) have been identified to be a potentially promising biomarker for diagnostic or prognostic use in numerous diseases as these fluids are easily accessible and the membrane of exosomes has protective effects that ensure more stable expression and higher diagnostic sensitivity [25,26]. Currently, the diagnosis of HSCR relies primarily on clinical manifestations combined with invasive procedures such as rectal biopsies, all of which have inherent limitations. These challenges highlight the urgent need for more reliable and, ideally, noninvasive diagnostic strategies [27].

In our previous study, we identified a panel of dysregulated exosomal miRNAs in HSCR plasma. Following multi-phase validation, five miRNAs were considered as potential diagnostic signatures, with miR-323a-3p showing notable diagnostic potential. Li et al. reported that miR-323a-3p could inhibit the proliferation and migration of bladder cancer cells by regulating epithelial-mesenchymal transition (EMT) [28]. In colorectal cancer, miR-323a-3p exhibited similar inhibitory effects on cell migration and also was proved to repress cell cycle progression [29].

Furthermore, we explored the correlation between TET2, a member of the TET family and a potential target gene of miR-323a-3p, and HSCR. TET2 (Ten-Eleven Translocation 2), as a classic DNA demethylase and tumor suppressor gene, has been widely

explored for its role in tumors, cardiovascular diseases, metabolic diseases, etc [30,31]. Emerging evidence indicates that TET protein silencing, particularly TET2 knockdown, disrupts neural differentiation and diminishes neurogenesis in mice [32,33]. Our results showed that TET2 expression was significantly reduced in HSCR colon tissues and that its downregulation was associated with impaired proliferative and migratory capacities of iENC. These findings, together with the regulatory relationship between miR-323a-3p and TET2, suggest that this axis may be involved in HSCR pathogenesis, although further studies are needed to confirm its precise role.

Building upon these results, our study provides preliminary evidence supporting the role of exosomal miR-323a-3p in HSCR pathogenesis through the TET2 axis. To further strengthen the causality and translational relevance of these findings, several important directions warrant future investigation. First, functional rescue experiments including both exosome depletion/repletion in cell models and in vivo delivery of engineered exosomes in relevant animal models, will be essential to directly validate the specific role of miR-323a-3p in neural colonization and phenotypic rescue. Second, spatial validation of miR-323a-3p expression and localization within human HSCR tissues using techniques such as RNA-FISH colocalization analysis could offer direct pathological insights and strengthen the clinical relevance of our observations. Together, these follow-up studies will help bridge our current mechanistic findings with potential clinical applications.

Up to today, where these HSCR-related plasma exosomes come from remains unknown. One possible origin is mesenchymal stem cells as such cells were reported to secrete exosomes that have neuroprotection effects [34,35]. Kumar et al. unearthed that exosomes derived from placenta mesenchymal stromal cells could increase cell number and neurites in a fetal lamb model and also suppress caspase activity of apoptotic SH-SY5Y [36]. In our previous study, we revealed that apoptotic neurons could inhibit the apoptosis of other cells by producing exosomes containing lncRNAs, which might suggest another potential source but requires further investigation [37].

At present, there remains a lack of robust, rapid, and physiologically relevant cellular for studying the enteric nervous system (ENS) in the context of HSCR. In the current study, we employed an immortalized ENCC-derived neural cell line (iENC), which retains certain key features of ENS progenitor cells but does not fully recapitulate the complexity or differentiation potential of native enteric neural precursors. To complement our in vitro findings, we utilized a zebrafish model carrying the Tg(HuC/D:tdTomato) transgene, in which red fluorescent protein tdTomato is expressed under the control of the HuC/D promoter. HuC/D is a well-characterized marker of post-mitotic neurons, broadly expressed in differentiated and mature neurons, but not exclusively specific to enteric neurons [38,39]. The tdTomato signal driven by the HuC/D promoter enables us to visualize the range of neuronal colonization in the intestinal region after the migration and differentiation of neural progenitor cells, although it cannot precisely or exclusively label intestinal neurons. Nevertheless, this model provided a useful platform for preliminary assessment of exosome effects on neural development and offered insights into the broader impact of miR-323a-3p and related pathways on ENS-associated cells.

5. Conclusion

This study shows that exosomal miR-323a-3p is significantly upregulated in HSCR and correlates with impaired proliferation and migration of enteric neural crest cells-derived neural cell lines. Our data suggested that miR-323a-3p may be involved in HSCR pathogenesis, potentially through downregulating TET2, a candidate downstream molecule requiring further functional characterization. The elevated exosomal miR-323a-3p levels in plasma may have diagnostic potential, although this requires further validation. Overall, our findings contributed to a better understanding of the molecular basis of HSCR and offer insights for future research.

Author contributions

Weibing Tang and Hongxing Li contributed to the Conceptualization, Resources, Supervision, Writing – Review & Editing. Xiurui Lv and Zichuan Gao contributed to the Resources and Data curation. Haoran Shen and Chenglong Wang contributed to the Investigation, Formal Analysis, Visualization and Writing – Original Draft. Yuanxiang Qiu, Zhengke Zhi and Jie Tang contributed to the Methodology and Writing – Review & Editing. Chunxia Du and Ruyi Zhang contributed to the Supervision and Project Administration.

Disclosure statement

The authors have no relevant affiliations or financial involvement with any organization or entity with a financial interest in or financial conflict with the subject matter or materials discussed in the manuscript. This includes employment, consultancies, honoraria, stock ownership or options, expert testimony, grants or patents received or pending, or royalties.

Reviewer disclosures

Peer reviewers on this manuscript have no relevant financial or other relationships to disclose.

Ethical declaration

This study was approved by Medical Ethics Committee of Children's Hospital Affiliated to Nanjing Medical University (Certification No:202411007-1). All procedures followed the Declaration of Helsinki, and written informed consent was obtained from all participants.

Data availability statement

All data supporting the research results can be obtained by the corresponding authors upon reasonable request.

Funding

This paper was not funded.

References

1. Montalva L, Cheng LS, Kapur R, et al. Hirschsprung disease. Nat Rev Dis Primers. 2023;9(1):54. doi: 10.1038/s41572-023-00465-y
2. Xu TO, Levitt MA, Feng C. Controversies in hirschsprung surgery. World J Pediatr Surg. 2024;7(3):e000887. doi: 10.1136/wjps-2024-000887
3. Verkuijl SJ, Friedmacher F, Harter PN, et al. Persistent bowel dysfunction after surgery for Hirschsprung's disease: a neuropathological

perspective. World J Gastrointest Surg. 2021;13(8):822–833. doi: 10.4240/wjgs.v13.i8.822
4. Sribudiani Y, Chauhan RK, Alves MM, et al. Identification of variants in RET and IHH pathway members in a large family with history of hirschsprung disease. Gastroenterology. 2018;155(1):118–129.e6. doi: 10.1053/j.gastro.2018.03.034
5. Holla Nd AM, Jehoul R, Vranken J, et al. MicroRNA regulation of enteric nervous system development and disease. Trends Neurosci. 2025;48(4):268–282. doi: 10.1016/j.tins.2025.02.004
6. Li Y, Zhou L, Lu C, et al. Long non-coding RNA FAL1 functions as a ceRNA to antagonize the effect of miR-637 on the down-regulation of AKT1 in Hirschsprung's disease. Cell Prolif. 2018;51(5):e12489. doi: 10.1111/cpr.12489
7. Xu Z, Yan Y, Gu B, et al. Up-regulation of microRNA-424 causes an imbalance in AKT phosphorylation and impairs enteric neural crest cell migration in hirschsprung disease. Int J Mol Sci. 2023;24(7). doi: 10.3390/ijms24076700
8. Peng L, Zhang H, Su Y, et al. Lipopolysaccharide enhances ADAR2 which drives Hirschsprung's disease by impairing miR-142-3p biogenesis. J Cell Mol Med. 2018;22(9):4045–4055. doi: 10.1111/jcmm.13652
9. Yeat NY, Chen RH. Extracellular vesicles: biogenesis mechanism and impacts on tumor immune microenvironment. J Biomed Sci. 2025;32(1):85. doi: 10.1186/s12929-025-01182-2
10. Kalluri R, LeBleu VS. The biology, function, and biomedical applications of exosomes. Science. 2020;367(6478). doi: 10.1126/science.aau6977
11. Gustafson CM, Roffers-Agarwal J, Gammill LS. Chick cranial neural crest cells release extracellular vesicles that are critical for their migration. J Cell Sci. 2022;135(12). doi: 10.1242/jcs.260272
12. Kinkade JA, Singh P, Verma M, et al. Small and long non-coding RNA analysis for human trophoblast-derived extracellular vesicles and their effect on the transcriptome profile of human neural progenitor cells. Cells. 2024;13(22). doi: 10.3390/cells13221867
13. Zhou Q, Yang L, Verne ZT, et al. Human colonic EVs induce murine enteric neuroplasticity via the lncRNA GAS5/miR-23/NMDA NR2B axis. JCI Insight. 2025;10(5). doi: 10.1172/jci.insight.178631
14. Lee YR, Kim G, Tak WY, et al. Circulating exosomal noncoding RNAs as prognostic biomarkers in human hepatocellular carcinoma. Int J Cancer. 2019;144(6):1444–1452. doi: 10.1002/ijc.31931
15. Li X, Wang Y, Wang Q, et al. Exosomes in cancer: small transporters with big functions. Cancer Lett. 2018;435:55–65. doi: 10.1016/j.canlet.2018.07.037
16. Lv X, Li Y, Li H, et al. Molecular function predictions and diagnostic value analysis of plasma exosomal miRNAs in Hirschsprung's disease. Epigenomics. 2020;12(5):409–422. doi: 10.2217/epi-2019-0190
17. Zhang Y, Liang S, Xiao B, et al. MiR-323a regulates ErbB3/EGFR and blocks gefitinib resistance acquisition in colorectal cancer. Cell Death Dis. 2022;13(3):256. doi: 10.1038/s41419-022-04709-9
18. Ge L, Habiel DM, Hansbro PM, et al. miR-323a-3p regulates lung fibrosis by targeting multiple profibrotic pathways. JCI Insight. 2016;1(20):e90301. doi: 10.1172/jci.insight.90301
19. Mousseau F, Berret JF, Oikonomou EK. Design and applications of a fluorescent labeling technique for lipid and surfactant preformed vesicles. ACS Omega. 2019;4(6):10485–10493. doi: 10.1021/acsomega.9b01094
20. Wang Q, Huang Z, Guo W, et al. microRNA-202-3p inhibits cell proliferation by targeting ADP-ribosylation factor-like 5A in human colorectal carcinoma. Clin Cancer Res. 2014;20(5):1146–1157. doi: 10.1158/1078-0432.Ccr-13-1023
21. Gontier G, Iyer M, Shea JM, et al. Tet2 rescues age-related regenerative decline and enhances cognitive function in the adult mouse brain. Cell Rep. 2018;22(8):1974–1981. doi: 10.1016/j.celrep.2018.02.001
22. Zou Z, Dou X, Li Y, et al. RNA m(5)C oxidation by TET2 regulates chromatin state and leukaemogenesis. Nature. 2024;634(8035):986–994. doi: 10.1038/s41586-024-07969-x
23. Trino S, Lamorte D, Caivano A, et al. Clinical relevance of extracellular vesicles in hematological neoplasms: from liquid biopsy to cell biopsy. Leukemia. 2021;35(3):661–678. doi: 10.1038/s41375-020-01104-1
24. Stahl PD, Raposo G. Extracellular vesicles: exosomes and Microvesicles, integrators of homeostasis. Physiology (Bethesda). 2019;34(3):169–177. doi: 10.1152/physiol.00045.2018
25. Merchant ML, Rood IM, Deegens JKJ, et al. Isolation and characterization of urinary extracellular vesicles: implications for biomarker discovery. Nat Rev Nephrol. 2017;13(12):731–749. doi: 10.1038/nrneph.2017.148
26. Jin X, Chen Y, Chen H, et al. Evaluation of tumor-derived exosomal miRNA as potential diagnostic biomarkers for early-Stage non-Small cell lung cancer using Next-generation sequencing. Clin Cancer Res. 2017;23(17):5311–5319. doi: 10.1158/1078-0432.Ccr-17-0577
27. Meinds RJ, Kuiper GA, Parry K, et al. Infant's age influences the accuracy of rectal suction biopsies for diagnosing of Hirschsprung's disease. Clin Gastroenterol Hepatol. 2015;13(10):1801–1807. doi: 10.1016/j.cgh.2015.04.186
28. Li J, Xu X, Meng S, et al. MET/SMAD3/SNAIL circuit mediated by miR-323a-3p is involved in regulating epithelial-mesenchymal transition progression in bladder cancer. Cell Death Dis. 2017;8(8):e3010. doi: 10.1038/cddis.2017.331
29. Bjeije H, Soltani BM, Behmanesh M, et al. YWHAE long non-coding RNA competes with miR-323a-3p and miR-532-5p through activating K-Ras/Erk1/2 and PI3K/Akt signaling pathways in HCT116 cells. Hum Mol Genet. 2019;28(19):3219–3231. doi: 10.1093/hmg/ddz146
30. Rasmussen KD, Berest I, Keβler S, et al. TET2 binding to enhancers facilitates transcription factor recruitment in hematopoietic cells. Genome Res. 2019;29(4):564–575. doi: 10.1101/gr.239277.118
31. Bowman RL, Levine RL. TET2 in normal and malignant hematopoiesis. Cold Spring Harb Perspect Med. 2017;7(8). doi: 10.1101/cshperspect.a026518
32. Verma N, Pan H, Doré LC, et al. Tet proteins safeguard bivalent promoters from de novo methylation in human embryonic stem cells. Nat Genet. 2018;50(1):83–95. doi: 10.1038/s41588-017-0002-y
33. Cakouros D, Hemming S, Gronthos K, et al. Specific functions of TET1 and TET2 in regulating mesenchymal cell lineage determination. Epigenet Chromatin. 2019;12(1):3. doi: 10.1186/s13072-018-0247-4
34. Fayazi N, Sheykhhasan M, Soleimani Asl S, et al. Stem cell-derived exosomes: a New strategy of neurodegenerative disease treatment. Mol Neurobiol. 2021;58(7):3494–3514. doi: 10.1007/s12035-021-02324-x
35. Jiang B, Yan L, Wang X, et al. Concise Review: mesenchymal stem cells derived from human pluripotent cells, an unlimited and quality-controllable source for therapeutic applications. STEM Cells. 2019;37(5):572–581. doi: 10.1002/stem.2964
36. Carney RP, Mizenko RR, Bozkurt BT, et al. Harnessing extracellular vesicle heterogeneity for diagnostic and therapeutic applications. Nat Nanotechnol. 2025;20(1):14–25. doi: 10.1038/s41565-024-01774-3
37. Du C, Xie H, Zang R, et al. Apoptotic neuron-secreted HN12 inhibits cell apoptosis in Hirschsprung's disease. Int J Nanomed. 2016;11:5871–5881. doi: 10.2147/ijn.S114838
38. Avila JA, Benthal JT, Schafer JC, et al. Single cell profiling in the Sox10(Dom) Hirschsprung Mouse implicates hox genes in enteric neuron trajectory allocation. Cell Mol Gastroenterol Hepatol. 2025;19(12):101590. doi: 10.1016/j.jcmgh.2025.101590
39. D'Errico F, Goverse G, Dai Y, et al. Estrogen receptor β controls proliferation of enteric glia and differentiation of neurons in the myenteric plexus after damage. Proc Natl Acad Sci USA. 2018;115(22):5798–5803. doi: 10.1073/pnas.1720267115